Robotica (2006) volume 24, pp. 257–268. © 2005 Cambridge University Press
doi:10.1017/S0263574705002109 Printed in the United Kingdom

# Quasi-human biped walking

Hun-ok Lim*†, Sang-ho Hyon‡, Samuel A. Setiawan‡ and Atsuo Takanishi†‡

(Received in Final Form: June 27, 2005, first published online 31 October 2005)

**SUMMARY**

Our goal is to develop biped humanoid robots capable of working stably in a human living and working space, with a focus on their physical construction and motion control. At the first stage, we have developed a human-like biped robot, WABIAN (WAseda BIped humANoid), which has a thirty-five mechanical degrees of freedom. Its height is 1.66 [m] and its weight 107.4 [kg]. In this paper, a moment compensation method is described for stability, which is based on the motion of its head, legs and arms. Also, a follow walking method is proposed which is based on a pattern switching technique. By a combination of both methods, the biped robot is able to perform dynamic stamping, walking forward and backward in a continuous time while someone is pushing or pulling its hand in such a way. Using WABIAN, human-fellow walking experiments are conducted, and the effectiveness of the methods are verified.

KEYWORDS: Interaction; Human-follow walking; Compensatory motion; Walking pattern; Pattern synthesis.

## I. INTRODUCTION

Biped humanoid robots intended to share the same working space with humans have different functional workability and maneuverability from conventional robots used in factories, construction fields or hazardous environments. Therefore, the mechanism, walking pattern and physical interaction of biped robots have received in recent years a particular attention. Especially, the mechanisms of biped robots have been studied by many researchers.[1–3] A biped walking robot, WL-10RD, was developed, and the dynamic walking was realized with the walking speed of 1.3 [s/step] on a plat ground, using the sequence control method.[4] One-, two-, and four-legged hydraulically actuated robots were developed, based on prismatic compliant legs.[5] A number of small electrically powered walking biped robots were built which balance using tabular control schemes.[6] The model of a five link planar biped robot that was controlled by using the state feedback was developed.[7] Recently, several research groups have been studying on the mechanism and control of biped walking robots.[8–10]

* Corresponding author. E-mail: holim@ieee.org
* Department of Mechanical Engineering, Kanagawa University 3-27-1 Rokkakubashi, Kanagawa-ku, Yokohama, 221-8686 (Japan).
† Humanoid Robotics Institute, Waseda University (Japan).
‡ Department of Mechanical Engineering, Waseda University (Japan).

Also, for the biped robots to behavior freely in a human living environment, motion pattern generation has been researched.[11–13] Based on the three-dimensional linear inverted pendulum mode, an online walking pattern generation was proposed.[14,15] Other researchers were studied on the motion patterns, based on the cooperation between an active sensor and a step sequence planner.[16]

In addition, the biped robots are strongly desired to have a flexible workability, such as doing along with human motion in physical contact. There are many studies that deal with physical interaction problems in human-robot coexistence.[17–19] The human-robot interaction was discussed using sensory and auditory information.[20] However, there are few reports on the realization of physical interaction between a human and a life-sized humanoid robot based on various action models. On the other hand, a physical interaction between humans may be realized by the action of shaking hands, walking together hand in hand, and even dancing. From these cases, it is reasonable to suppose that the hand has an important role in physical interactions with humans. Thus, under the circumstances of human-robot coexistence, our purpose for this research is to realize a locomotive following motion by a biped humanoid robot to human motion by hand contact.

In this paper, we describe how to compensate for moments generated by the motion of the legs and arms. Also, how to classify unit patterns for follow walking is discussed. To let a biped robot follow human guidance motion, a follow walking method is proposed. This method contains three parts; (1) an upper-limb (arm) following control method, to let the hand of the biped robot follow to the direction of the guidance motion, (2) a lower-limb trajectory planning method, to let the biped robot walk (or just marking time) in the direction of its guidance motion, and (3) a trunk trajectory planning method, to compensate for the moment generated by the upper- and lower-limbs. The human-follow walking methodl employs a switching pattern technique generating and selecting unit patterns based on the action model for human-robot interaction. Also, the method calculates the joint trajectories, including the trunk trajectory for the compensation of various motion patterns.

This paper is organized as follows. In section II, we describe a moment compensation method to cancel moments generated by a biped locomotion. Section III describes an arm follow motion to follow human motion by hand contact. Section IV discusses a follow walking method based on pattern-switching technique. Section V illustrates the mechanism of a biped humanoid robot and experimental results. Finally, Section VI provides conclusions.

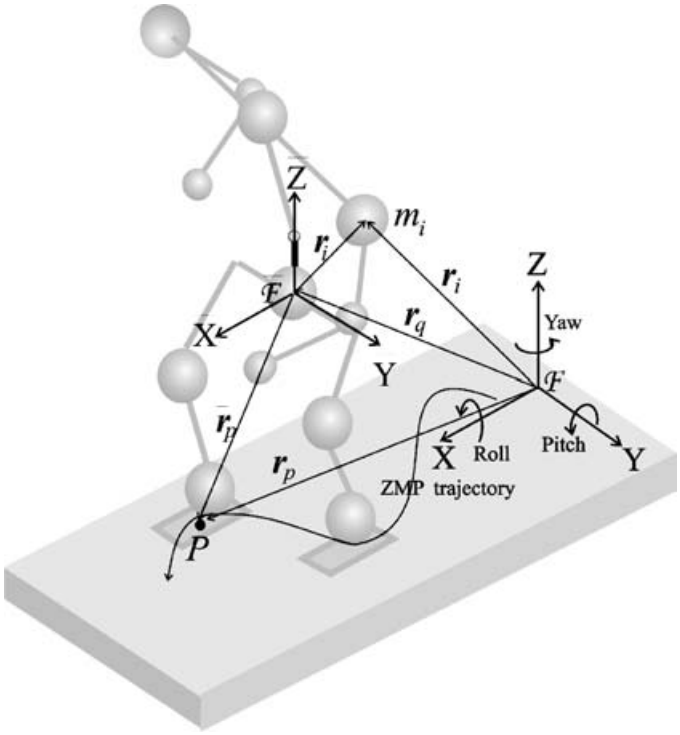


Fig. 1. Coordinate frames.

## II. MOMENT COMPENSATION BY TRUNK AND WAIST MOTION

A moment compensation for stability is described in this section, which is an improved version of a model based control already proposed by us.[21] This control method computes the compensatory trunk motion from the motion of the lower-limbs and upper-limbs and the time trajectory of ZMP planned arbitrarily before walking.

### *II.1. Coordinate frames*

We consider a 35-DOF biped humanoid model with rotational joints that consists of two 3-DOF legs, two 7-DOF arms, two 3-DOF hands, a 2-DOF neck, two 2-DOF eyes and a torso with a 3-DOF trunk. To define mathematical quantities, a world coordinate frame $\mathcal{F}$ is fixed on the floor where the biped robot can walk as shown in Figure 1. Also, a moving coordinate frame $\bar{\mathcal{F}}$ is attached on the center of the waist on a parallel with the world coordinate frame $\mathcal{F}$ in consideration of the relative motion of each particle. To specify the dynamic behavior of the biped model, five assumptions are also defined as follows:

(i) the biped robot consists of a set of particles,
(ii) the foothold of the biped robot is rigid and not moved by any force and moment,
(iii) the contact region between the foot and the floor surface is a set of contact points,
(iv) the coefficients of friction for rotation around the X, Y and Z-axes are nearly zero at the contact point between the feet and the floor surface, and
(v) the feet of the robot do not slide on the contact surface.

### *II.2. Derivation of trunk motion*

By assuming that the upper-limbs are one part of the trunk, we can define an approximation model of the trunk and the

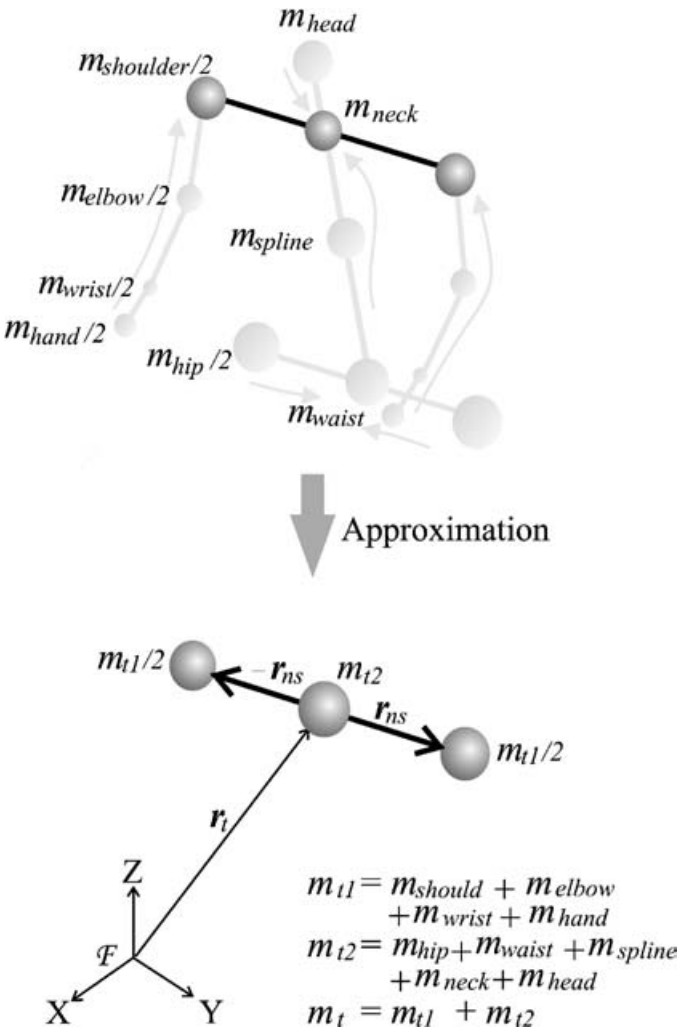


Fig. 2. Approximation model of the upper-body.

position vectors as shown Figure 2. Based on this model, the moment balance around a point $P$ on the floor can be written as below:

$$m_{t1}\boldsymbol{r}_{ns} \times \ddot{\boldsymbol{r}}_{ns} + \sum_{i=1}^{n} m_i(\boldsymbol{r}_i - \boldsymbol{r}_p) \times (\ddot{\boldsymbol{r}}_i + \boldsymbol{G}) + \boldsymbol{T} = \boldsymbol{0} \quad (1)$$

where $m_{t1}$ denotes the mass of the arms and shoulders ($m_{t1} = m_{shoulder} + m_{elbow} + m_{wrist} + m_{hand}$). $\boldsymbol{r}_{ns}$ is the position vector of the shoulder. $\boldsymbol{r}_p$ is the position vector of the point $p$ with respect to $\mathcal{F}$. $m_i$ is the mass of the particle $i$. $\boldsymbol{r}_i$ and $\ddot{\boldsymbol{r}}_i$ denote the position and acceleration vectors of the particle $i$ with respect to $\mathcal{F}$, respectively. $\boldsymbol{G}$ is the gravitational acceleration vector. $\boldsymbol{T}$ is the moment vector acting on the contact point $p$.

Let ZMP be on the point $P$. The moment $\boldsymbol{T}$ is zero according to the ZMP concept. By putting the terms about the motion of the upper-limb particles on the left-hand side as unknown variables, and the terms about the moment generated by the lower-limb particles on the right-hand side as known parameters, $\boldsymbol{M} = [M_x\ M_y\ M_z]^T$, Equation (1) can be modified and expanded as follows with respect

https://doi.org/10.1017/S0263574705002109 Published online by Cambridge University Press

to $\bar{\mathcal{F}}$:

$$m_{t1}(z_{ns}\ddot{x}_{ns} - x_{ns}\ddot{z}_{ns}) + m_t(\bar{z}_t + z_q)(\ddot{\bar{x}}_t + \ddot{x}_q) - m_t(\ddot{\bar{z}}_t + \ddot{z}_q + g_z)(\bar{x}_t - \bar{x}_{zmp}) = -M_y, \quad (2)$$

$$m_{t1}(y_{ns}\ddot{z}_{ns} - z_{ns}\ddot{y}_{ns}) - m_t(\bar{z}_t + z_q)(\ddot{\bar{y}}_t + \ddot{y}_q) + m_t(\ddot{\bar{z}}_t + \ddot{z}_q + g_z)(\bar{y}_t - \bar{y}_{zmp}) = -M_x, \quad (3)$$

$$-m_{t1}(x_{ns}\ddot{y}_{ns} - y_{ns}\ddot{x}_{ns} + M_{yt}) = -M_z, \quad (4)$$

where

$$M_{yt} = -m_t(\ddot{\bar{x}}_t + \ddot{x}_q)(\bar{y}_t - \bar{y}_{zmp}) + m_t(\ddot{\bar{y}}_t + \ddot{y}_q)(\bar{x}_t - \bar{x}_{zmp}) \quad (5)$$

where $m_t$ denotes the total mass of the head, neck, waist, arms and hips. $\bar{\boldsymbol{r}}_t = [\bar{x}_t\ \bar{y}_t\ \bar{z}_t]^T$ is the position vector of the neck with respect to $\bar{\mathcal{F}}$. $\bar{\boldsymbol{r}}_{zmp} = [\bar{x}_{zmp}\ \bar{y}_{zmp}\ 0]^T$ is the position vector of ZMP with respect to $\bar{\mathcal{F}}$. $\boldsymbol{r}_q = [x_q\ y_q\ z_q]^T$ is the position vector of the origin of the moving frame $\bar{\mathcal{F}}$ from the origin of $\mathcal{F}$. $M_{zt}(t)$ is the yaw moment generated by the motion of the trunk.

However, these Equations (2), (3), (4) and (5) are interferential and non-linear, because each equation has the same variable, $\bar{z}_t$, and the trunk is connected to the lower-limbs by rotational joints. Therefore, it is difficult to derive analytic solutions from them. By assuming that neither the waist nor the trunk particles move vertically, and the trunk arm rotates on the horizontal plane only, the equations can be decoupled and linearized as follows:

$$m_t(\bar{z}_t + z_q)(\ddot{\bar{x}}_t + \ddot{x}_q) - m_t g_z(\bar{x}_t - \bar{x}_{zmp}) = -M_y, \quad (6)$$

$$-m_t(\bar{z}_t + z_q)(\ddot{\bar{y}}_t + \ddot{y}_q) - m_t g_z(\bar{y}_t - \bar{y}_{zmp}) = -M_x, \quad (7)$$

$$m_{t1}R_t^2\ddot{\theta}_y = M_{yt} - M_z, \quad (8)$$

where $\theta_y$ is the rotational angle of the yaw-axis of the trunk and $R_t$ is the radius of the trunk's arm.

In the above Equations (6), (7) and (8), the moments $M_y$, $M_x$, and $M_z$ are known because they are derived from the motion of the lower-limbs and the time trajectory of ZMP. Also, the yaw-axis moment generated by the trunk motion, $M_{yt}$, is derived from the pitch and roll-axis motion of the trunk. In the case of steady walking, $M_y$, $M_x$, and $M_z$ are periodic functions because each particle of the lower-limbs and the time trajectory of ZMP move periodically with respect to the moving coordinate frame $\bar{\mathcal{F}}$ . Thus, each equation can be represented as a Fourier series. By comparing the Fourier Transform coefficients from both sides of each equation, we can easily acquire the approximate periodic solution for the motion of the trunk. To determine an offset term in the equation of the yaw-axis moment, we take into consideration that the generated yaw-motion angle is in the range of the rotatable region of the yaw-axis actuator.

This method is also applicable to a complete walking that starts from static standing state and returns to a static standing state again. By regarding the whole complete walking motion as one periodic walking motion and applying the method to it, the compensatory motion of the trunk for steady and transitional walking can be derived. Then, it is necessary to have a long period of standing time before starting motion and after stopping motion.

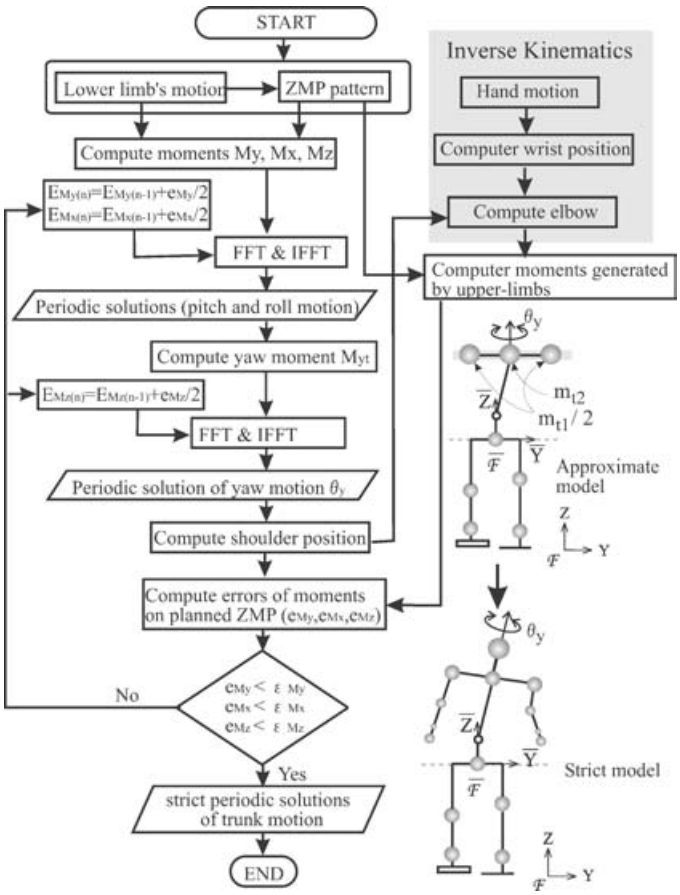


Fig. 3. Flow chart to compute trunk motion.

Furthermore, in order to obtain strict solutions, an algorithm computing the approximate solutions iteratively is used. The flowchart of the algorithm is shown in Figure 3. These computations are repeated until moment errors between moments calculated by the planned ZMP and by the motion of the trunk fall below a certain tolerance level, $\boldsymbol{\epsilon} = [\epsilon_{My}\ \epsilon_{Mx}\ \epsilon_{Mz}]^T$. However, this method needs a huge number of iterations in computation. So, through the use of computation regularity, we estimate the limit value of an accumulated moment error on each axis as follows:

$$\boldsymbol{E}_n = \frac{2\boldsymbol{E}_{n-1} + \boldsymbol{e}_{n-1}}{2} \quad (9)$$

where $\boldsymbol{E}_n = [E_{My}\ E_{Mx}\ E_{Mz}]^T$ is the accumulated moment error in the $n$th iteration, and $e_n$ is the calculated moment error after $n$ times of iteration.

As a consequence, we realized about a 90 percent decrease in the number of iteration times.

## III. ARM FOLLOW MOTION

A virtual compliance control is employed to let the robot's arm follow human motion by hand contact. In this research, we adopt a conventional compliance method.[22] To determine the motion of the upper-limb, a shoulder coordinate frame $\mathcal{F}_s$ is attached on the center of the shoulder, and a hand coordinate frame $\mathcal{F}_h$ is established on the center of the hand.

https://doi.org/10.1017/S0263574705002109 Published online by Cambridge University Press

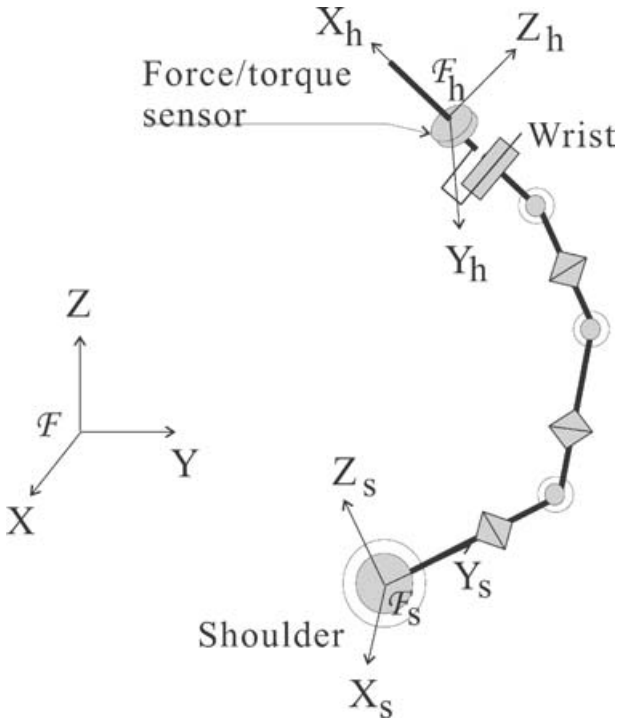


Fig. 4. The arm model for follow motion.

A force/torque sensor is attached between the hand and the wrist to measure forces applied to the hand. Figure 4 shows the coordinate systems of the upper-limb. The equation of compliance motion of the robot'hand can be written by

$$\boldsymbol{M}\frac{d\boldsymbol{v}_h}{dt} = \boldsymbol{F}_h - \boldsymbol{K}\Delta\boldsymbol{x}_h - \boldsymbol{C}\boldsymbol{v}_h, \tag{10}$$

where $\boldsymbol{M} \in \Re^{6\times6}$ is the virtual mass matrix. $\boldsymbol{K} \in \Re^{6\times6}$ and $\boldsymbol{C} \in \Re^{6\times6}$ are the stiffness and damping matrices, respectively. $\boldsymbol{F}_h \in \Re^6$ is the external force vector acting on the robot hand. $\boldsymbol{v}_h \in \Re^6$ and $\Delta\boldsymbol{x}_h \in \Re^6$ is the velocity and deviation vectors of the robot's hand, respectively.

In the case where our target is the full tracking ability of the hand, like the method generally used in the direct teaching of an industrial manipulator, the stiffness components may be disregarded. Also, when the control loop time we apply is very short (5 [ms]), we may think of the virtual mass as equal to zero. Therefore, Equation (11) can be rewritten as

$$\boldsymbol{v}_h = \boldsymbol{C}^{-1}\boldsymbol{F}_h. \tag{11}$$

The velocity of the hand can be expressed with respect to the shoulder frame $\mathcal{F}_s$ as follows:

$${}^s\boldsymbol{v}_h = {}^s\boldsymbol{R}_h\ \boldsymbol{v}_h, \tag{12}$$

where ${}^s\boldsymbol{R}_h$ is the hand rotation matrix with respect to the frame $\mathcal{F}_s$.

According to the redundancy of the arm, we used the pseudo-inverse matrix $\boldsymbol{J}^+$ to calculate the desired joint angle velocity of the arm $\dot{\boldsymbol{\theta}}_d \in \Re^7$ from the hand velocity ${}^s\boldsymbol{v}_h$. Thus, the joint angle velocity of the arm is written as follows:

$$\dot{\boldsymbol{\theta}}_d = \boldsymbol{J}^+\,{}^s\boldsymbol{v}_h, \tag{13}$$

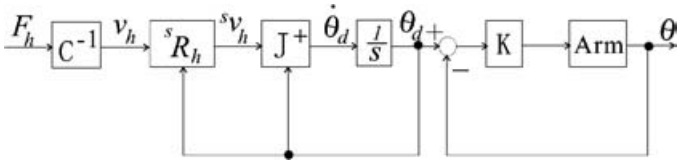


Fig. 5. Control system for the follow motion of the arm.

where

$$\boldsymbol{J}^+ = \boldsymbol{J}^T(\boldsymbol{J}\boldsymbol{J}^T)^{-1}$$

where $\boldsymbol{J}$ is $6 \times 7$ Jacobian matrix.

Figure 5 shows a control system for the follow motion of the upper-limb. Using Equation (14), each desired joint angle of the arm is calculated to realize the follow motion of the upper-limb by hand contact.

## IV. HUMAN-FOLLOW WALKING

In order to realize human-follow walking motion by a biped robot, a human-follow walking method with a pattern-switching technique is discussed in this section. This method tries to realize a follow-walking motion by generating and selecting changeable unit patterns, based on an action model of human-robot interaction. Note that the selectable unit patterns are calculated offline and kept in the computer memory. We here will describe the making of unit patterns and decision for the following direction in this section.

### *IV.1. Constructing unit patterns*

Two men who adjust their motion to one another while moving on the ground, have various gaits while in action. They walk freely in a two-dimensional space, and switch their step or velocity half unconsciously to follow their partner's motion. It is difficult to apply all motion patterns to a biped robot. However, by combining some of the selective patterns, it is possible to realize a following motion by a biped robot similar to a human's.

By considering that the biped model has only pitch degree of freedom on its lower-limb, in this research, we only made back and forth (including marking in place) motion patterns for realizing the human-follow motion. However, it can be easily extended to another kind of two-dimensional motion, including sideways or diagonal motions.

There are various numbers of gait patterns even in a back-and-forth motion, and those have a countless number of classification methods. However, notice that we can plan the lower-limb motion arbitrarily, while we can only decide the trunk trajectory due to consideration of the dynamical condition of balance of the robot. We are able to make and classify various kinds of motion patterns from the observation explained in the next section. The pattern generation of the low-limbs can be found in our previous study.[13]

### *IV.2. Classification of lower-limb's unit patterns*

By defining a step of back-and-forth walking as a unit pattern, we classify the motion of each leg into five types of step motion in consideration of the locomotive motion velocity (a gait attribute per a step) as shown in Figure 6.

Basically, the human-follow motion by the combination of these types of step motions has been realized. To prevent

https://doi.org/10.1017/S0263574705002109 Published online by Cambridge University Press

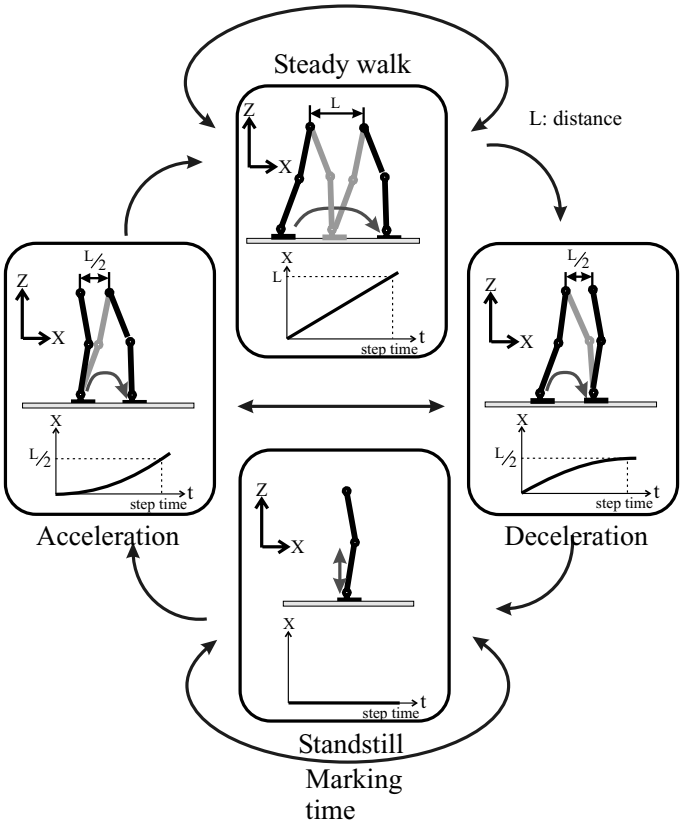


Fig. 6. 5 types of lower-limb's motion.

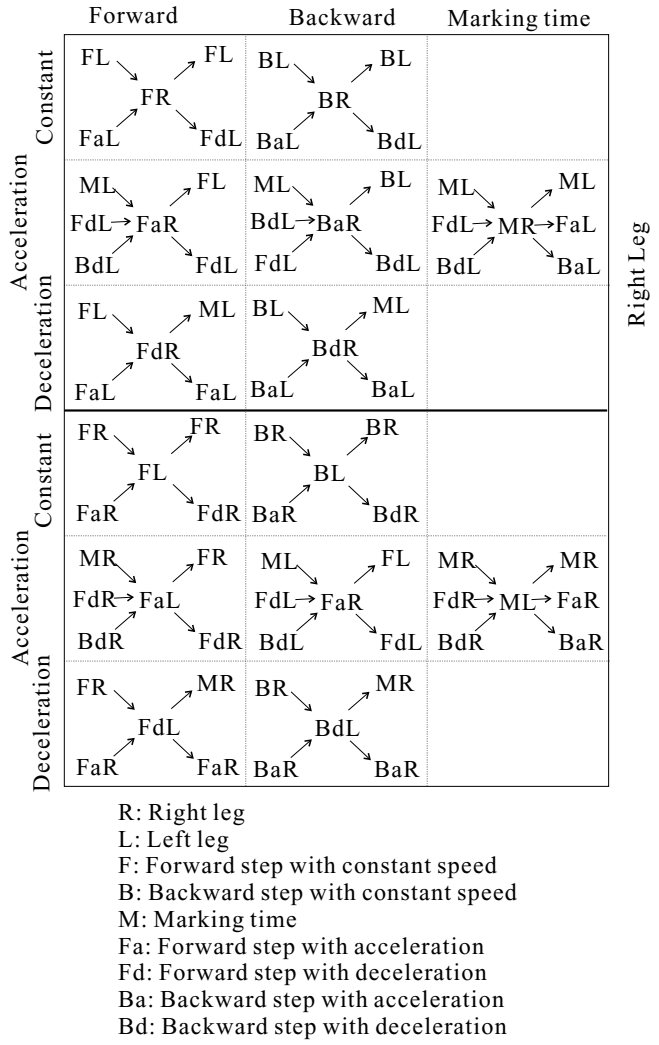


R: Right leg
L: Left leg
F: Forward step with constant speed
B: Backward step with constant speed
M: Marking time
Fa: Forward step with acceleration
Fd: Forward step with deceleration
Ba: Backward step with acceleration
Bd: Backward step with deceleration

Fig. 7. Connection rule of unit patterns.

instability in the motion of the trunk (see the next section) caused by an excessive change of moment around the ZMP, we decided that the lower-limb unit patterns must be performed mutually in the direction of the arrow as shown in Figure 6. The connection rule for the unit patterns is shown in Figure 7. The unit patterns are generated by a polynomial.[13]

*IV.3. Classification of trunk unit patterns*

To compensate for the moments generated by the motion of the lower-limb planned above, the motion of the trunk is used. In section 2, we have described how to obtain the compensatory motion of the trunk. In this section, the unit pattern of the trunk is discussed.

It has been noted that in classifying unit patterns of the trunk, the dynamics of the motion of the trunk should be considered. The equation of moment balance around the pitch and roll axis, Equation (6) and Equation (7) can be changed as

$$(\bar{z}_t + z_q)\ddot{\bar{x}}_t - g_z\bar{x}_t = A(t), \tag{14}$$

$$(\bar{z}_t + z_q)\ddot{\bar{y}}_t - g_z\bar{y}_t = B(t), \tag{15}$$

where

$$A(t) = \frac{-M_y(t) - m_t(\bar{z}_t + z_q)\ddot{x}_q - m_t g_z \bar{x}_{zmp}}{m_t},$$
$$B(t) = \frac{M_y(t) - m_t(\bar{z}_t + z_q)\ddot{y}_q - m_t g_z \bar{y}_{zmp}}{m_t}, \tag{16}$$

where $A(t)$ and $B(t)$ are known valuables of Equation (6) and Equation (7).

Consider only the motion of the trunk around the pitch axis to investigate the compensatory motion. The transfer function $\bar{y}_t(\omega)$ in the frequency domain can be expressed as

$$\bar{y}_t(\omega) = \frac{2p}{\omega^2 + p^2}q = \left(\frac{1}{p - j\omega} + \frac{1}{p + j\omega}\right)q, \tag{17}$$

where

$$p = \sqrt{\frac{g_z}{\bar{z}_t - \bar{z}_{zmp}}}, \qquad q = -\frac{1}{2g_z}\sqrt{\frac{g_z}{\bar{z}_t - \bar{z}_{zmp}}}. \tag{18}$$

According to the ZMP concept, $\bar{z}_{zmp}$ in Equation (19) is zero. Equation (18) is generally known as Lorentz function, and its primitive function is written as

$$\bar{y}_t(t) = qe^{-p|t|}. \tag{19}$$

We can imagine from Equation (19) that the casual law may not be applied anymore. It should be clear that the trunk compensation motion occurs earlier than the shift of ZMP on the floor. Also, it means that the trunk compensation gives effect to one or more steps before and after in a pattern time. The frequency of the trunk moment is higher as the biped robot moves faster. Therefore, the effect of $\bar{y}_t(\omega)$ is more dominant in a fast motion.

https://doi.org/10.1017/S0263574705002109 Published online by Cambridge University Press

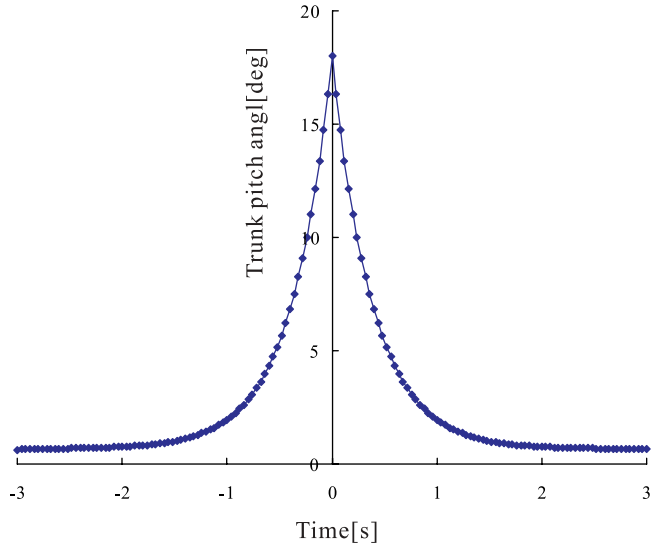


Fig. 8. Compensatory motion of the trunk.

To confirm the trunk motion, an impulse moment 1000[Nm] is applied to the pitch trunk when a biped robot is not in motion. Figure 8 shows the pitch motion of the trunk. In this simulation, we can see that the compensatory motion of the trunk should be begun with a view of balancing before and after the impulse moment is applied to the biped robot.

Using two different walking patterns, the deviation of the trunk motion is simulated. A pattern A consists of steady 6-step walking with a forward step only, but a pattern B unsteady 6-step including backward steps as shown in Figure 9. Figure 10 shows the compensatory angle trajectory and angular velocity of the trunk motion of pattern A and pattern B at four different walking speeds. We can see that the trajectories diverge and then converge again because two walking patterns have the same gate in their first and sixth step. Also, we can see that the diversion and conversion points are different depending on the walking speed. In a slow walking, the trajectories diverse at the second step time point, but in a fast walking, the diversion has already occurred from around the first step time point as shown in Figure 10. It means that a total unit pattern increases in the fast walking, because the unit pattern of the trunk must consider the gait attribute one step before and after. Therefore, we decide to make the unit pattern of the trunk to deal with the step time of 1.0 [s/step] in this study.

From the walking simulations, we have confirmed that it is possible to make a unit pattern for the trunk by taking into account only one step before and after as an attribute. By using our simulator, one hundred ten unit patterns of the lower-limb and trunk are made based on the consideration above. The unit patterns create contain indexes for pattern searching and attributes of steps current, before and after as shown in Figure 11. For example, the pattern A can be made combining the unit patterns as follows: $2(3) \rightarrow 56 \rightarrow 30 \rightarrow 77 \rightarrow 6 \rightarrow 41(43)$. These patterns are preloaded as one step long angle data in the memory.

### *IV.4. Decision of following direction*

In this section, we will discuss a topic equivalent to a part of the action model in human physical interaction. That is a

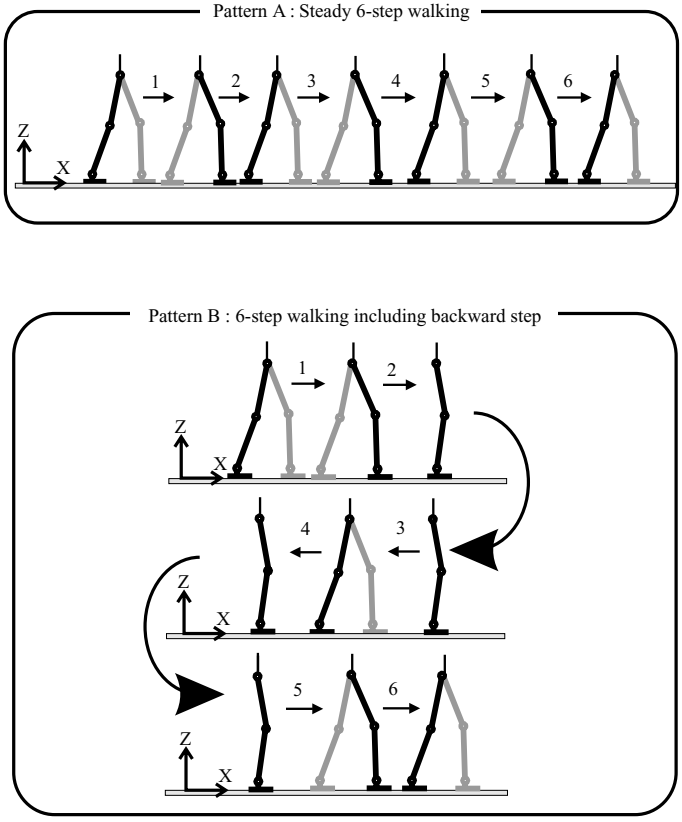


Fig. 9. Two different walking patterns.

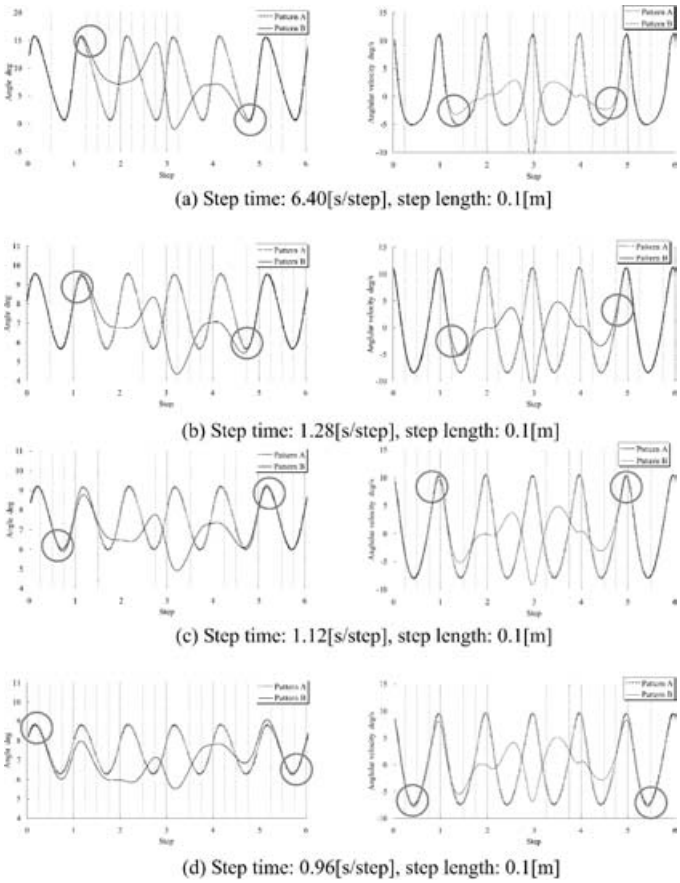


Fig. 10. Simulation results: the circles denote the diverging and converging areas.

https://doi.org/10.1017/S0263574705002109 Published online by Cambridge University Press

I

| | P | C | N |
|---|---|---|---|
| 0 | FL | FR | FL |
| 1 | FaL | FR | FL |
| 2 | FL | FR | FdL |
| 3 | FaL | FR | FdL |

II

| | P | C | N |
|---|---|---|---|
| 4 | ML | FaR | FL |
| 5 | FdL | FaR | FL |
| 6 | BdL | FaR | FL |
| 7 | S | FaR | FL |
| 8 | ML | FaR | FdL |
| 9 | FdL | FaR | FdL |
| 10 | BdL | FaR | FdL |
| 11 | S | FaR | FdL |

III

| | P | C | N |
|---|---|---|---|
| 12 | FL | FdR | ML |
| 13 | FaL | FdR | ML |
| 14 | FL | FdR | FaL |
| 15 | FaL | FdR | FaL |
| 16 | FL | FdR | BaL |
| 17 | FaL | FdR | BaL |
| 18 | FL | FdR | S |
| 19 | FaL | FdR | S |

IV

| | P | C | N |
|---|---|---|---|
| 20 | BL | BR | BL |
| 21 | BaL | BR | BL |
| 22 | BL | BR | BdL |
| 23 | BaL | BR | BdL |

V

| | P | C | N |
|---|---|---|---|
| 24 | ML | BaR | BL |
| 25 | BdL | BaR | BL |
| 26 | FdL | BaR | BL |
| 27 | S | BaR | BL |
| 28 | ML | BaR | BdL |
| 29 | BdL | BaR | BdL |
| 30 | FdL | BaR | BdL |
| 31 | S | BaR | BdL |

VI

| | P | C | N |
|---|---|---|---|
| 32 | BL | BdR | ML |
| 33 | BaL | BdR | ML |
| 34 | BL | BdR | BaL |
| 35 | BaL | BdR | BaL |
| 36 | BL | BdR | FaL |
| 37 | BaL | BdR | FaL |
| 38 | BL | BdR | S |
| 39 | BaL | BdR | S |

VII

| | P | C | N |
|---|---|---|---|
| 40 | FR | FL | FR |
| 41 | FaR | FL | FR |
| 42 | FR | FL | FdR |
| 43 | FaR | FL | FdR |

VIII

| | P | C | N |
|---|---|---|---|
| 44 | MR | FaL | FR |
| 45 | FdR | FaL | FR |
| 46 | BdR | FaL | FR |
| 47 | S | FaL | FR |
| 48 | MR | FaL | FdR |
| 49 | FdR | FaL | FdR |
| 50 | BdR | FaL | FdR |
| 51 | S | FaL | FdR |

IX

| | P | C | N |
|---|---|---|---|
| 52 | FR | FdL | MR |
| 53 | FaR | FdL | MR |
| 54 | FR | FdL | FaR |
| 55 | FaR | FdL | FaR |
| 56 | FR | FdL | BaR |
| 57 | FaR | FdL | BaR |
| 58 | FR | FdL | S |
| 59 | FaR | FdL | S |

X

| | P | C | N |
|---|---|---|---|
| 60 | BR | BR | BR |
| 61 | BaR | BR | BR |
| 62 | BR | BR | BdR |
| 63 | BaR | BR | BdR |

XI

| | P | C | N |
|---|---|---|---|
| 64 | MR | BaL | BR |
| 65 | BdR | BaL | BR |
| 66 | FdR | BaL | BR |
| 67 | S | BaL | BR |
| 68 | MR | BaL | BdR |
| 69 | BdR | BaL | BdR |
| 70 | FdR | BaL | BdR |
| 71 | S | BaL | BdR |

XII

| | P | C | N |
|---|---|---|---|
| 72 | BR | BdL | MR |
| 73 | BaR | BdL | MR |
| 74 | BR | BdL | BaR |
| 75 | BaR | BdL | BaR |
| 76 | BR | BdL | FaR |
| 77 | BaR | BdL | FaR |
| 78 | BR | BdL | S |
| 79 | BaR | BdL | S |

XIII

| | P | C | N |
|---|---|---|---|
| 80 | ML | FaR | FL |
| 81 | FdL | FaR | FL |
| 82 | BdL | FaR | FL |
| 83 | S | FaR | FL |
| 84 | ML | FaR | FdL |
| 85 | FdL | FaR | FdL |
| 86 | BdL | FaR | FdL |
| 87 | S | FaR | FdL |
| 88 | FL | FdR | ML |
| 89 | FaL | FdR | ML |
| 90 | FL | FdR | FaL |
| 91 | FaL | FdR | FaL |
| 92 | FL | FdR | BaL |
| 93 | FaL | FdR | BaL |
| 94 | FL | FdR | S |

XIV

| | P | C | N |
|---|---|---|---|
| 95 | ML | BaR | BL |
| 96 | BdL | BaR | BL |
| 97 | FdL | BaR | BL |
| 98 | S | BaR | BL |
| 99 | ML | BaR | BdL |
| 100 | BdL | BaR | BdL |
| 101 | FdL | BaR | BdL |
| 102 | S | BaR | BdL |
| 103 | BL | BdR | ML |
| 104 | BaL | BdR | ML |
| 105 | BL | BdR | BaL |
| 106 | BaL | BdR | BaL |
| 107 | BL | BdR | FaL |
| 108 | BaL | BdR | FaL |
| 109 | BL | BdR | S |

P: Previous step, C: Current step
N: Next step, S: standstill
M: Marking time
R: Right leg, L: Left leg
F: Forward step with constant speed
B: Backward step with constant speed
Fa: Forward step with acceleration
Fd: Forward step with deceleration
Ba: Backward step with acceleration
Bd: Backward step with deceleration

(a) (b) (c)

Fig. 11. 110 Unit walking patterns. (a) Unit pattern 0 to unit pattern 39. (b) Unit pattern 40 to unit pattern 79. (c) Unit pattern 80 to unit pattern 109.

process where a robot recognizes human intention, and then decides to start an action as a response.

Under the circumstances of interaction between a human and his/her partner, including the surrounding environment, there is a mapping process (an action model of a behavioral pattern) between the conditions of three elements that change depending on the time and action to be performed. Based on this consideration, we determine an action model to realize the interaction between a human and a biped robot as shown in Figure 12. In this model, the robot recognizes the guiding direction of the human to move by detecting the position or displacement of its hand, and decides the next walking pattern while synchronizing it with the present walking condition. In the case of where no pattern is selected, we program to let the present condition be continued by the robot.

## V. EXPERIMENTS

We have demonstrated human-follow walking in this section. The hardware and software of the experimental system are described briefly, and the experimental results are presented.

### *V.1. Hardware and software*

To explore follow-walking motion, a biped humanoid robot with a human configuration, WABIAN, has been constructed as shown in Figure 13. The WABIAN consists of a total of thirty-five mechanical degrees of freedom (DOF); two 3-DOF legs, two 7-DOF arms, two 3-DOF hands, a 2-DOF neck, two 2-DOF eyes and a torso with a 3-DOF trunk as shown in Figure 14. The height of the WABIAN is about 1.66 [m] and its total weight is 107.4 [kg]. Table I illustrates the mass distribution of the WABIAN.

Duralumin, GIGAS (YKK Corporation) and CFRP (Carbon Fiber Reinforced Plastic) are mainly employed as structural materials of the WABIAN. The body and legs are driven by AC servo motors with reduction gears. The neck, hands and arms are actuated by DC servo motors with reduction gears, but the eyes by DC servo motors without reduction gears. A force/torque sensor is used to detect interaction, which is attached on the wrist.

The WABIAN is controlled by a PC/AT compatible computer PEAK-530 (Intel MMX Pentium 200 MHz CPU

Table 1. Mass parameters of WABIAN.

| Parts | Weight [kg] | Parts | Weight [kg] |
|---|---|---|---|
| Foot | 1.1 (×2) | Hand | 0.4 (×2) |
| Ankle | 6 (×2) | Wrist | 0.5 (×2) |
| Knee | 5.2 (×2) | Elbow | 0.9 (×2) |
| Head | 2.4 | Shoulder | 6 (×2) |
| Neck | 6.4 | Waist | 18.3 |
| Trunk | 40.1 | | |

https://doi.org/10.1017/S0263574705002109 Published online by Cambridge University Press

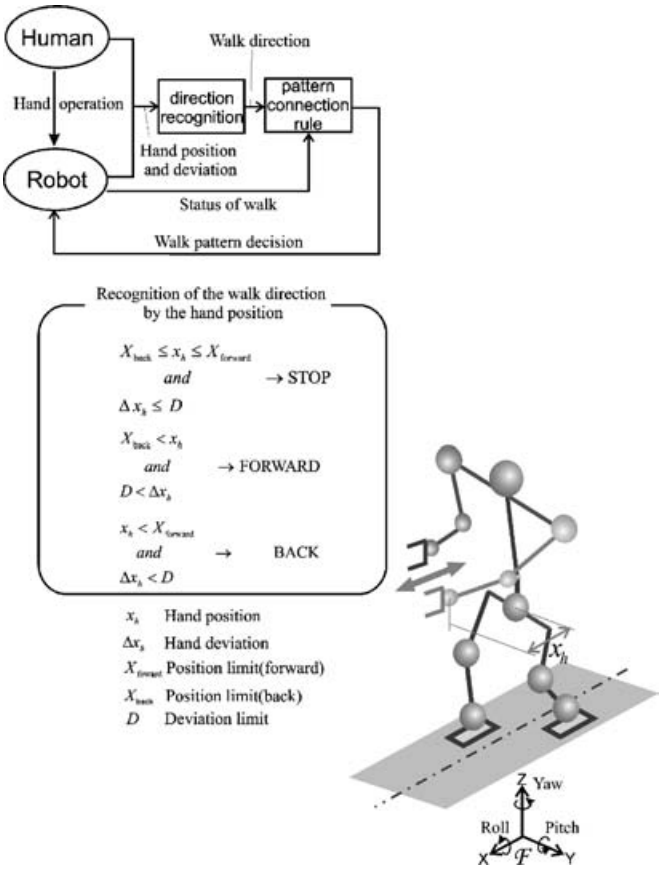


Fig. 12. Human-robot interaction model.

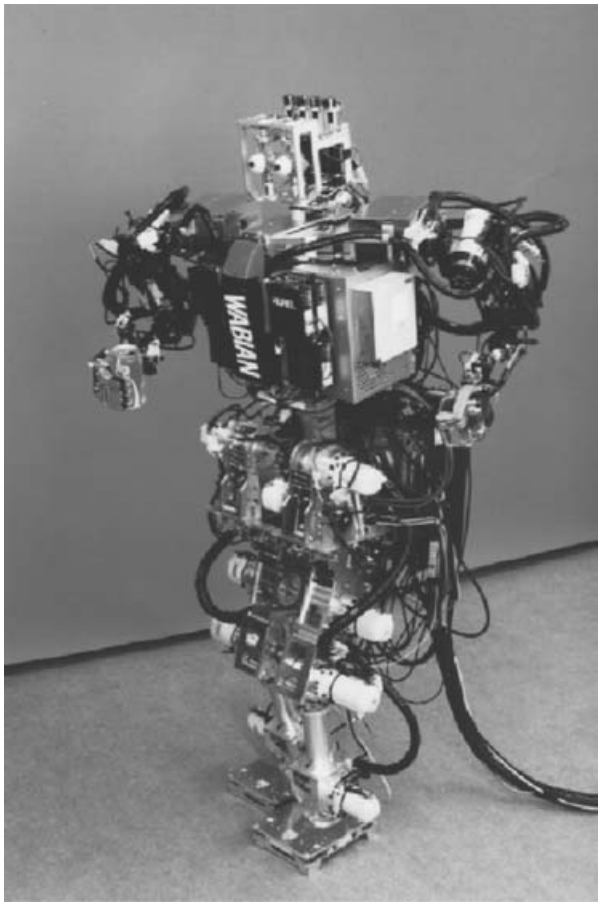


Fig. 13. Photo of WABIAN.

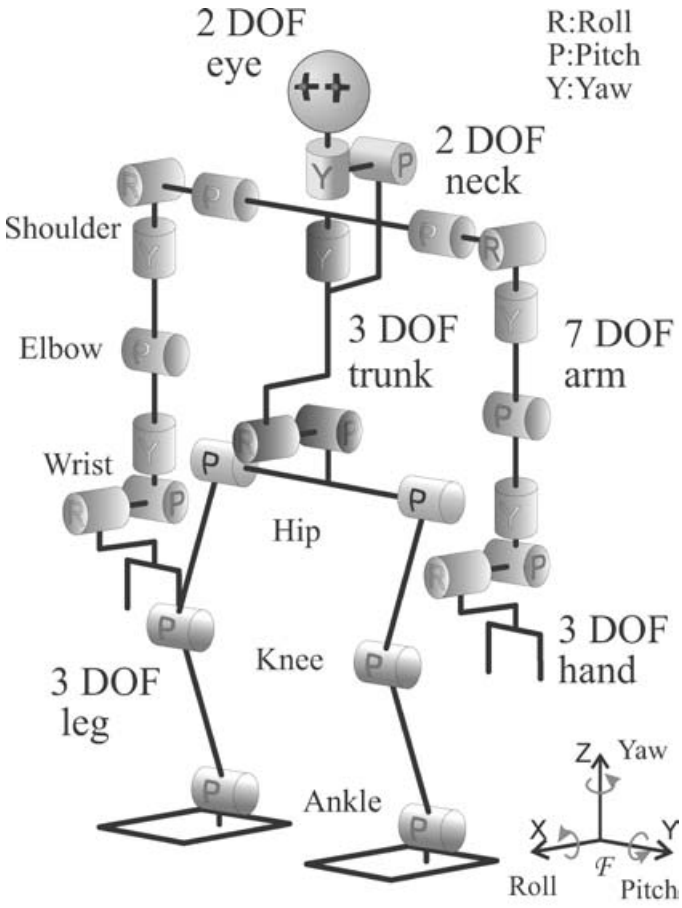


Fig. 14. DOF of WABIAN.

processor) with MS-DOS 6.2/V (16-bit). TNT DOS-Extender SDK (Ver.6.1) is employed to produce a 32-bit operation system. It has three counter boards with each 24-bit 24 channels, three D/A converter boards with each 12-bit 16 channels and an A/D converter board with differential 12-bit 16 channels to interface with sensors. The joint angles are sensed by incremental encoders attached at the joints, and the data are taken to the computer through the counters. All the computations to control the WABIAN are carried out by the control computer and the control program is written in C language. The servo rate is 1 kHz. The computer system is mounted on the back of the waist and the servo driver modules are mounted on the upper part of the trunk. The external connection is only an electric power source.

*V.2. Experimental procedure and results*

Using the WABIAN, a human-follow walking experiment with 12 steps is conducted. To let its right arm to able to follow a human's guidance through a hand, the damping coefficient of the virtual compliance arm model is selected as $\boldsymbol{C} = diag(0.7, 0.7, 0.7, 0.7, 0.7, 0.7)$. The forward position limit is selected as $X_{\text{forward}} = 0.3$, the backward position limit $X_{\text{back}} = 0.1$, and the deviation limit $D = 0.15$ to determine the walking direction. Also, the step velocity is 1.28 [s/step], and the step width is 0.1 [m/step].

The experimental schemes are as follows: (i) the five types unit patterns of the lower-limbs are planned arbitrarily according to the walking direction before walking, (ii) the

https://doi.org/10.1017/S0263574705002109 Published online by Cambridge University Press

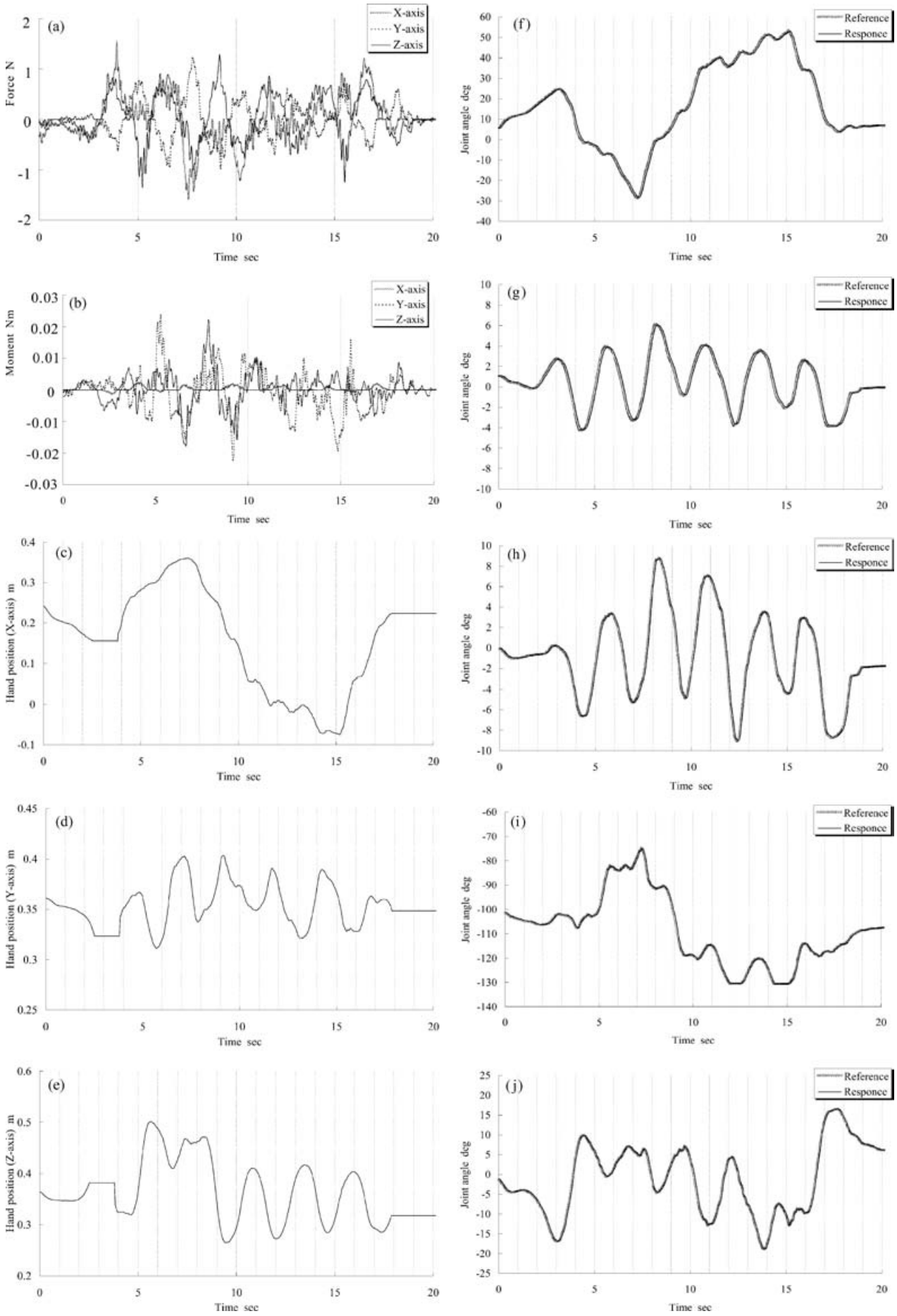


Fig. 15. For caption see next page.

https://doi.org/10.1017/S0263574705002109 Published online by Cambridge University Press

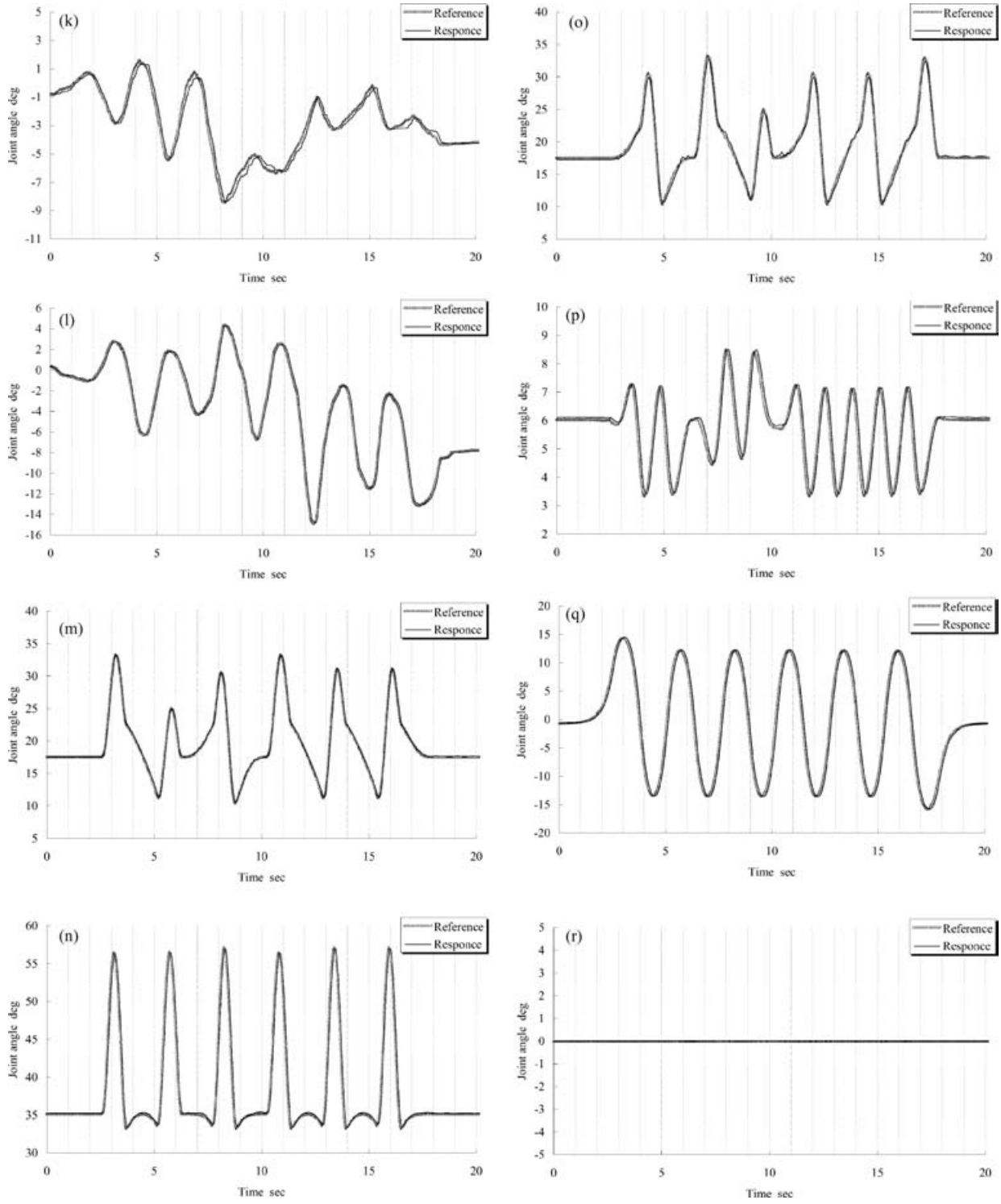


Fig. 15. Experimental results in human-follow walking experiment with 16 steps. (a) Force applied to the right hand. (b) Moment applied to the right hand. (c) X position of the right hand. (d) Y position of the right hand. (e) Z position of the right hand. (f) Pitch angle of the right shoulder. (g) Roll angle of the right shoulder. (h) Yaw angle of the right shoulder. (i) Pitch angle of the right elbow. (j) Pitch angle of right wrist. (k) Roll angle of the right wrist. (l) Yaw angle of the right wrist. (m) Pitch angle of the right ankle. (n) Pitch angle of the right knee. (o) Pitch angle of the right hip. (p) Pitch angle of the trunk. (q) Roll angle of the trunk. (r) Yaw angle of the trunk.

compensatory unit patterns of the trunk are calculated by the moment compensation method for the balance of the biped robot, (iii) these unit patterns are preloaded as angle data in the computer memory of the biped robot, and (iv) depending on the pattern connection rule and the walking direction determined by interaction model, the unit patterns (i) and (ii) are selected online.

Figure 15 (a) and (b) show measured forces and moments applied to the right hand of the WABIAN, respectively. Depending on the applied forces, the pitch, roll and yaw positions of the hand are shown in Figure 15 (c), (d) and (e), respectively. Figure 15 (f), (g), (h), (i), (j), (k) and (l) show the joint responses of the right shoulder, elbow and wrist, respectively. Figure 15 (m), (n) and (o) show the joint

https://doi.org/10.1017/S0263574705002109 Published online by Cambridge University Press

responses of the right pitch ankle, knee and hip, respectively. Figure 15 (p), (q) and (r) show the pitch, roll and yaw joint responses of the trunk, respectively. In this experiment, we can see that the reference patterns of the lower-limbs are selected according to the follow direction, and are followed very well. Also, we can see that the pitch and roll trunk begin to move at about 2.5 [s] and 0.5 [s], respectively, as shown in Figure 15 (p) and (q), while the joints of the right leg start to move at around 2.7 [s] as shown in Figure 15 (m), (n) and (o). It means that the trunk motion compensates for the moments generated as the trunk moves earlier than the lower-limbs during the follow walking. In this study, the yaw motion of the trunk is considered for the balance of the WABIAN as shown in Figure 15 (r). If the trunk begins to move later than the movement of the lower-limb, the biped robot will be unstable and fall down because of the dynamic behavior of the biped robot (see Section IV). These results clarify that the moment compensation method and human-follow walking method are effective for human-follow motion.

From the experimental results, we will be able to realize not only an advanced interactive motion but also a teaching playback, if we make more various patterns. If we define the rule of the motion of the lower-limbs from the motion of both hands, we also will be able to teach a dance to the biped robot.

## VI. CONCLUSION AND DISCUSSION

To realize physical interaction between a human and a life-size humanoid robot, two methods were presented which is based on an action model. A moment compensation method was discussed which compensates for moments generated by the motion of the lower-limbs, upper-limbs using the motion of the trunk. For the balance of the robot body, the trunk motion should be considered one step before and after. Also, a follow-walking method was described to let the biped humanoid robot follow human guidance motion through hand contact. This method generates unit patterns of five types and switches them considering the pattern connection rule and the walking direction. To confirm the methods, WABIAN having 35-DOF was developed, and follow walking experiments were conducted and realized. While someone is pushing or pulling its hand, it walks forward and backward and marks time during a continuous time.

It is difficult to achieve fellow walking with higher speed (below 1 [s/step]) because the unit pattern is considered only one step before and after. To solve this, more steps should be considered before and after the change of the unit pattern, and the landing time should be changed. This will be our future work. To realize more stable walking, not only a compliance control of the lower-limbs capable of reducing impact forces should be introduced into the lower-limbs, and the combined motion of the trunk and the waist should be employed for stability. These will be future problems to be solved.

For more advanced interactive motion, various unit patterns should be generated online and dynamically changed according to the human robot interaction. This work will be introduced in another paper.

**Acknowledgement**

This study has been conducted as a part of the humanoid project at Humanoid Robotics Institute, Waseda University. This study was funded in part by JSPS under Japanese grant-in-aid for Scientific Research and NEDO (New Energy and Industrial Technology Development Organization). The authors would also like to thank NITTA Corp, OKINO Industries Ltd., Harmonic Drive Systems, Inc., YKK Corp, Daisuke AOYAGI and Akihiro NAGAMATSU for supporting us in developing the hardware.

## References

1. H. Hemami and B. F. Wyman, "Modeling and control of constrained dynamics systems with application to biped locomotion in the frontal plane," *IEEE Trans. Automatic Control*, **24**, 526–535 (1992).
2. J. Furusho and M. Masubuchi, "Control of a dynamical biped locomotion system for steady walking," *ASME J. Dynamics Systems, Measurement, and Control*, **108**, 111–118 (June, 1986).
3. S. Kajita and K. Tani, "Study of dynamic biped locomotionon rugged terrain: Theory and basic experiment," *Proc. Int. Conf. Advanced Robotics*, Sacramento, CA (Apr., 1991), pp. 741–746.
4. A. Takanishi, M. Ishida, Y. Yamazaki and I. Kato, "The realization of dynamic walking by the biped walking robot," *Proc. IEEE Int. Conf. Robotics and Automation*, St. Louis, MO (Mar., 1985), pp. 459–466.
5. M. H. Raibert, *Legged Robots That Balance* (MIT Press, Cambridge, MA, 1986).
6. H. Miura and I. Shimoyama, "Dynamic walk of a biped," *Int. J. Robotics Research*, **3**, No. 2, 60–74 (Summer, 1984).
7. R. L. Farnsworth and H. Hemami, "Postural and gait stability of a planar five link biped by simulation," *IEEE Trans. Automatic Control*, **22**, No. 3, 452–458 (June, 1977).
8. K. Hirai, M. Hirose, Y. Haikawa and T. Takenaka, "The development of honda humanoid robot," *Proc. IEEE Int. Conf. Robotics and Automation,* Leuven, Belgium (May, 1998), pp. 1321–1326.
9. K. Nishiwaki, S. Kagami, Y. Kuniyoshi, M. Inaba and H. Inoue, "Online generation of humanoid walking motion based on a fast generation method of motion pattern that follows desired zmp," *Proc. IEEE/RSJ Int. Conf. Intelligent Robots and Systems*, Lausanne, Switzerland (Oct., 2002), pp. 2684–2689.
10. K. Kaneko, F. Kanehiro, S. Kajita, K. Yokoyama, K. Akachi, T. Kawasaki, S. Ota and T. Isozumi, "Design of prototype humanoid robotics platform for hrp," *Proc. IEEE/RSJ Int. Conf. Intelligent Robots and Systems*, Lausanne, Switzerland (Oct., 2002), pp. 2431–2436.
11. F. M. Silva and J. A. Machado, "Towards efficient biped robots," *Proc. IEEE/RSJ Int. Conf. Intelligent Robots and Systems* (1998), pp. 394–399.
12. P. H. Channon, S. H. Hopkins and D. T. Phan, "Derivation of optimal walking motions for a biped walking robot," *Robotica*, **10**, Part 2, 165–172 (1992).
13. H. O. Lim and A. Takanishi, "Walking pattern generation for biped locomotion," *Int. Symp. Robotics*, Seoul, Korea (Apr., 2001), pp. 1551–1556.
14. S. Kajita, F. Kanehiro, K. Kaneko, K. Fujiwara, K. Yokoi and H. Hirukawa, "A realtime pattern generator for biped walking," *Proc. IEEE Int. Conf. Robotics and Automation*, Washington, D.C. (May, 2002), pp. 31–37.
15. T. Sugihara, Y. Nakamura and H. Inoue, "Realtime humanoid motion generation through zmp manipulation based on inverted pendulum control," *Proc. IEEE Int. Conf. Robotics and Automation*, Washington, D.C. (May, 2002), pp. 1404–1409.
16. O. Lorch, A. Albert, J. Denk, M. Gerecke, R. Cupec, J. Seara, W. Gerth and G. Schmidt, "Experiments in vision-guided biped

walking," *Proc. IEEE/RSJ Int. Conf. Intelligent Robots and Systems*, Lausanne, Switzerland (Sept., 2002), pp. 2484–2490.
17. H. Kazerooni, "Human-robot interaction via the transfer of power and information signals," *IEEE Trans. Systems, Man, and Cybernetics*, **20**, No. 2, 450–463 (1990).
18. I. D. Walker, "Impact configurations and measures for kinematically redundant and multiple armed robot systems," *IEEE Trans. Robotics and Automation*, **10**, No. 5, 670–683 (1994).
19. Z. C. Lin, R. V. Patel and C. A. Balafoutis, "Impact reduction for redundant manipulators using augmented impedance control," *J. Robotic Systems*, **12**, No. 5, 301–313 (1995).
20. Y. Ogura, Y. Sugahara, Y. Kaneshima, N. Hieda, H. O. Lim and A. Takanishi, "Interactive biped locomotion based on visual/auditory information," *Proc. IEEE Int. Workshop Robot and Human Communication*, Berlin, Germany (Sept., 2002), pp. 253–258.
21. J. Yamaguchi, A. Takanishi and I. Kato, "Development of a biped walking robot compensating for three-axis moment by trunk motion," *Proc. IEEE/RSJ Int. Conf. Intelligent Robots and Systems*, Yokohama, Japan (July, 1993), pp. 561–566.
22. M. T. Mason, "Compliance and force control for computer controlled manipulators," *IEEE Trans. Systems, Man, and Cybernetics*, **11**, No. 6, 418–432 (June, 1981).

https://doi.org/10.1017/S0263574705002109 Published online by Cambridge University Press